Toxicology and Applied Pharmacology 370 (2019) 117–130

Contents lists available at ScienceDirect

Toxicology and Applied Pharmacology

journal homepage: www.elsevier.com/locate/taap

The protective role of spermine against male reproductive aberrations induced by exposure to electromagnetic field – An experimental investigation in the rat

Nancy N. Shahin[a,*], Nagla A. El-Nabarawy[b], Ahmed S. Gouda[b], Bruno Mégarbane[c,d]

[a] Department of Biochemistry, Faculty of Pharmacy, Cairo University, Cairo, Egypt
[b] National Egyptian Center of Environmental and Toxicological Research (NECTER), Faculty of Medicine, Cairo University, Cairo, Egypt
[c] INSERM UMRS-1144, Paris-Diderot University, Paris, France
[d] Department of Medical and Toxicological Critical Care, Lariboisière Hospital, Paris, France

ARTICLE INFO

Keywords:
Electromagnetic field
Steroid sex hormone
Spermine
Sperm profile
Testis
Toxicity

ABSTRACT

The exponentially increasing use of electromagnetic field (EMF)-emitting devices imposes substantial health burden on modern societies with particular concerns of male infertility. Limited studies have addressed the modulation of this risk by protective agents. We investigated the hazardous effects of rat exposure to EMF (900 MHz, 2 h/day for 8 weeks) on male fertility and evaluated the possible protective effect of the polyamine, spermine, against EMF-induced alterations. Exposure to EMF significantly decreased sperm count, viability and motility, and increased sperm deformities. EMF-exposed rats exhibited significant reductions in serum inhibin B and testosterone along with elevated activin A, follicle-stimulating hormone, luteinizing hormone and estradiol concentrations. Testicular steroidogenic acute regulatory protein (StAR), c-kit mRNA expression and testicular activities of the key androgenic enzymes 3β- and 17β-hydroxysteroid dehydrogenases were significantly attenuated following exposure to EMF. Exposure led to testicular lipid peroxidation, decreased catalase and glutathione peroxidase activities and triggered nuclear factor-kappa B p65, inducible nitric oxide synthase, cyclooxygenase-2 and caspase-3 overexpression. EMF-exposed rats showed testicular DNA damage as indicated by elevated comet parameters. Spermine administration (2.5 mg/Kg/day intraperitoneally for 8 weeks) prevented EMF-induced alterations in the sperm and hormone profiles, StAR and c-kit expression and androgenic enzyme activities. Spermine hampered EMF-induced oxidative, inflammatory, apoptotic and DNA perturbations. Histological and histomorphometric analysis of the testes supported all biochemical findings. In conclusion, rat exposure to EMF disrupts sperm and hormone profiles with underlying impairment of steroidogenesis and spermatogenesis. Spermine confers protection against EMF-associated testicular and reproductive aberrations, at least in part, *via* antioxidant, anti-inflammatory and anti-apoptotic mechanisms.

1. Introduction

A broad spectrum of electromagnetic waves is nowadays emitted by a variety of natural and man-made sources of electromagnetic field (EMF). With the extensive use of EMF-generating devices including cell phones, > 3 billion people worldwide are daily exposed (Fragopoulou et al., 2010). The global system for mobile communications operating at 850–900 and 1850–1990 MHz frequency bands is the most extensively applied system for mobile telecommunications worldwide (Sepehrimanesh et al., 2014a; Valberg et al., 2007). According to this system, 900 MHz is of the most widely used frequency bands (Eghlidospour et al., 2017; Wu and Razavi, 1998). The mean age of starting mobile phone use has rapidly dropped to elementary school age with alarmingly increasing durations of exposure to EMF (Manikonda

Abbreviations: 3β-HSD, 3β-hydroxysteroid dehydrogenase; 17β-HSD, 17β-hydroxysteroid dehydrogenase; COX-2, cyclooxygenase-2; EMF, electromagnetic field; FSH, follicle stimulating hormone; GAPDH, Glyceraldehyde-3-phosphate dehydrogenase; GSH, glutathione; GPx, glutathione peroxidase; H&E, hematoxylin and eosin; iNOS, inducible nitric oxide synthase; LH, luteinizing hormone; MDA, malondialdehyde; M-MuLV, Moloney Murine Leukemia Virus; NAD+, nicotinamide adenine dinucleotide; NADP+, nicotinamide adenine dinucleotide phosphate; NF-κB, nuclear factor-kappa B; ODC1, ornithine-decarboxylase-1; PAS, periodic acid Schiff stain (PAS); qRT-PCR, quantitative real-time polymerase chain reaction; StAR, steroidogenic acute regulatory protein; STBM, seminiferous tubule basement membrane; STD, seminiferous tubule diameter

* Corresponding author.
E-mail address: nancy.shahin@cu.edu.eg (N.N. Shahin).

https://doi.org/10.1016/j.taap.2019.03.009
Received 5 November 2018; Received in revised form 25 February 2019; Accepted 12 March 2019
Available online 13 March 2019
0041-008X/ © 2019 Elsevier Inc. All rights reserved.

et al., 2007). Therefore, long-term exposure to EMF has become the focus of extensive researches due to the risk of critical alterations in biological systems.

EMF penetration into the testis is likely more prominent in comparison to other tissues due to its anatomical and histological structure (Kesari et al., 2011). Based on the high susceptibility of male reproductive organs to environmental hazards, attention has been drawn to the consequences of exposure to EMF, but reports are controversial yet (Bilgici et al., 2018; Dasdag et al., 2003; Kesari et al., 2011; Kesari and Behari, 2012). Additionally, only scarce studies have addressed the possible modulation of EMF-induced testicular and reproductive aberrations by effective agents.

Polyamines including spermine are intimately implicated in reproduction and embryo-fetal development (Lefèvre et al., 2011). Normal testicular polyamine levels seem crucial for reproductive function (Pegg, 2014). Spermine is one of the natural semen components and under normal physiological conditions protects sperm DNA. Interestingly, antioxidant, anti-inflammatory and anti-apoptotic effects have been attributed to spermine in different models of tissue injury (Motawi et al., 2007; Paul and Kang, 2013; Abu-Khudir et al., 2017).

We thus designed this experimental study to investigate the potential hazardous effects of exposure to EMF on male rat fertility and evaluate the protective effect of spermine against EMF-induced testicular and reproductive alterations. In our study, the effect of EMF exposure and its possible modulation by spermine were evaluated in terms of key determinants of male fertility. Morphometric alterations were detected by measuring seminiferous tubule diameter, basement membrane thickness and seminiferous tubule epithelial height. Sperm count, viability, motility and morphology were assessed as sensitive indicators of sperm production and quality. Serum reproductive hormones, follicle stimulating hormone (FSH), luteinizing hormone (LH), inhibin B, activin A, testosterone and estradiol, were determined to evaluate the pituitary-gonadal axis functioning. Steroidogenic acute regulatory protein (StAR), 3β and 17β-hydroxysteroid dehydrogenases (3β-HSD and 17β-HSD) were estimated as key determinants of steroidogenesis and androgenesis, respectively, whereas c-kit was assayed as a marker of spermatogenesis. Oxidative stress, inflammation and apoptosis were investigated as possible underlying mechanisms for elucidating the effects of EMF exposure and spermine administration.

2. Methods

All experimental procedures complied with the Guide for the Care and Use of Laboratory Animals published by the US National Institutes of Health (NIH Publication No. 85–23, revised 2011) and were approved by the Institutional Animal Care and Use Committee of Cairo University (Approval number: CU-III-F-43-17).

2.1. Animals

The study was conducted on 32 adult male Wistar rats (180–220 g, 6–7 weeks old) obtained from the laboratory animal farm of the Egyptian Organization for Biological Products and Vaccines and housed in a 12-h light/dark cycle, at a 60 ± 10% humidity and 25 ± 2.0 °C temperature with access *ad libitum* to water and standard rodent chow diet.

2.2. Chemicals

Spermine tetrahydrochloride (Sigma-Aldrich Chemical Co., St. Louis, MO, US) was dissolved in saline (NaCl 0.9%) and administered intraperitoneally at 2.5 mg/Kg/day dose during eight consecutive weeks, as previously described (Wei et al., 2016). All other chemicals used were of analytical grade.

2.3. Exposure to EMF

The EMF-producing device included a radiofrequency signal generator (Aeroflex 2025, Testwall Ltd., UK), two monopole antennas, a power amplifier (Stealth Microwave SM 0520–36, SSB Technologies Inc., NJ, US) and a field survey meter (frequency from 0 to 4 GHz, EMF 200, Narda, Germany). Rats were placed in a circular plastic tray (50-cm diameter), divided into equal sectors to ensure equal exposure to radiation. The antenna was fixed in the center of the tray. To avoid stress, an aperture (1.5-cm diameter) was provided in the upper lid of each sector tip toward the antenna to allow rats breathing. This design makes the non-restrained rats freely directed toward the radiation antenna (Mohammed et al., 2013; Paffi et al., 2013). Rats were exposed to the EMF at 900 MHz frequency and 0.02 mW/cm^2 power density during 2 h/day over a period of eight consecutive weeks, as previously described (Kesari et al., 2011). The average specific absorption rate was 1.075 W/Kg, as calculated by the Finite-Difference-Time-Domain. Non-exposed rats were placed in the same device with exposure off, used in similar environmental conditions.

2.4. Experimental design

After a one-week acclimatization period, rats were randomly allocated into four groups ($N = 8$ rats/group) to receive saline (5 mL/Kg/day) or spermine tetrahydrochloride (2.5 mg/Kg/day) intraperitoneally (before the exposure session) during 8 consecutive weeks with concomitant exposure to EMF during 2 h/day (EMF and EMF + SP groups, respectively) or not (control and SP groups, respectively).

2.5. Sample preparation

Rats were sacrificed by decapitation under thiopental anesthesia, 24 h after the last dose. Immediately after decapitation, blood was collected. Serum was separated for the determination of inhibin B, activin A, gonadotrophin and steroid sex hormone levels. Pairs of epididymides and testes were rapidly excised, rinsed in saline and blot dried. The epididymides were used for the determination of sperm count, motility, viability and morphology. The right testis was fixed in 10%-buffered formalin/saline for 72 h for histological, histomorphometric and immunohistochemical analyses. The left testis was divided into three parts. The first part was homogenized in ice-cold bidistilled water to give a 10%-homogenate. An aliquot of the homogenate was mixed with Tris-HCl buffer (0.01 mol/L, pH 7.4) and ultracentrifuged at 10,000 g at 4 °C for 30 min. The resulting supernatant was used to determine the activities of the antioxidant enzymes glutathione peroxidase (GPx) and catalase, the key enzymes of testicular androgenesis, 3β-HSD and 17β-HSD as well as the testicular protein level. Another aliquot of the homogenate was mixed with 2.3% KCl, centrifuged at 600*g* and the resulting supernatant was used to determine the level of malondialdehyde (MDA), an end-product of lipid peroxidation. The second part of the left testis was stored at −80 °C for the determination of StAR and c-kit gene expression levels by quantitative real-time polymerase chain reaction (qRT-PCR). The third portion of the left testis was placed in phosphate-buffered saline (PBS) and stored at −80 °C for the DNA damage evaluation.

2.6. Histologic, histomorphometric and immunohistochemical analyses

Ten percent formalin-fixed testicular tissue samples were trimmed and processed by dehydration in alcohol, clearing in xylene, synthetic wax infiltration and blocking out into Paraplast tissue embedding medium. Five μm thick sections were cut by a rotatory microtome. The obtained sections were stained with hematoxylin and eosin (H&E) for histopathological examination through the light microscope, and with periodic acid Schiff stain (PAS) for demonstration of the seminiferous tubule basement membrane (STBM) thickness, as outlined by Bancroft

and Gamble (2008).

Five non-overlapping fields were randomly selected in each section for the determination of the seminiferous tubule diameter (STD) and germinal epithelium height in the H&*E*-stained sections, and for the determination of the STBM thickness in the PAS-stained sections. Morphological measurements were analyzed and photographs were taken using Leica Application Suite attached to Full HD microscopic imaging system (Leica Microsystems GmbH, Germany).

For the determination of nuclear factor-kappa B (NF-κB) p65, cyclooxygenase-2 (COX-2), inducible nitric oxide synthase (iNOS), and caspase-3 immunoexpression in the germinal epithelium, immunohistochemical staining of 5 μm-thick paraffin-embedded tissue sections was performed. Briefly, deparaffinized tissue sections were treated with 0.03% H_2O_2 for 20 min followed by incubation with rabbit anti-rat antibodies for NF-κB p65, COX-2, iNOS and caspase-3 (Catalog #: RB-1638-P0 (1:100), RB-9072-P0 (1:150), RB-9242-P0 (1:100) and RB-1197-P0 (1:150), respectively, Thermo Fisher Scientific, CA, US) for 30 min at room temperature. After washing, the sections were incubated with a secondary antibody-horseradish peroxidase EnVision kit (Dako, Copenhagen, Denmark) for 20 min, washed with PBS and incubated with 3,3′-diaminobenzidine (Dako, Copenhagen, Denmark) for 10 min. After PBS washing, the slides were counterstained with hematoxylin, dehydrated, cleared in xylene and visualized using a digital camera installed on a Leica DMLB2 light microscope (Leica Microsystems, Germany). Ten non-overlapping fields (400×) were randomly selected in each section and fractions of diaminobenzidine-positive immunoreactive area were automatically calculated as area percentage of immunopositive cells to the total area of the microscopic field using image analysis software (Leica QWin Plus V3, Leica Microsystems Ltd., Switzerland).

2.7. Assessment of epididymal sperm parameters

Epididymal sperm count and motility were assessed by a modified method of Ernst (1989). Briefly, the entire epididymis was removed, cut longitudinally to expose the epididymal coils, then 5–6 transverse cuts were made along the length of the organ and the spermatozoa were flushed out with 2 mL saline. The sperm suspension was then transferred to a hemocytometer for the assessment of motility and count under 40×-magnification. Evaluation of motility was accomplished within 30 min of sperm isolation from the cauda, after which the sperm number was determined. The sperm suspension was then smeared and stained with eosin-nigrosin to evaluate sperm viability and morphology under 400×-magnification. Sperm viability was determined by assessing the live/dead ratio. For morphological assessment, a sperm was classified as being of normal morphology if it had a hook-shaped head and no defects of head, neck or tail. Otherwise, sperms were considered abnormal (Rato et al., 2013).

2.8. Determination of serum hormone levels

Serum concentrations of FSH, LH, testosterone and estradiol were determined using ELISA kits (Catalog #: KT-59859, KT-60294, KT-60838 and KT-59814, respectively), according to the manufacturer's protocols (Kamiya Biomedical Company, Seattle, WA, US). The FSH and LH ELISA assays employed a quantitative sandwich immunoassay, whereas the testosterone and estradiol ELISA kits applied the competitive enzyme immunoassay technique. Briefly, serum was incubated with horseradish peroxidase (HRP)-conjugated polyclonal antibody specific for the hormone (in FSH and LH assays) or with a hormone-HRP conjugate (in testosterone and estradiol assays) in a microtiter plate pre-coated with an anti-hormone antibody.

Serum inhibin B and activin A concentrations were measured using RayBio® kits (Catalog #: EIAR-INB and ELR-ActivinA, respectively), according to the manufacturer's instructions (RayBiotech, Norcross, GA, US). The inhibin B enzyme immunoassay adopted the competitive enzyme immunoassay principle whereby a biotinylated inhibin B peptide was spiked into the serum samples (in the ratio of 1:1), which were then incubated with an anti-inhibin B antibody in the plate. The activin A assay employed a sandwich-based ELISA in which the serum (diluted 1:3) was incubated with a biotinylated anti-rat activin A antibody in a plate pre-coated with an antibody specific for activin A. After washing, HRP-streptavidin was applied to interact with the bound biotinylated component in each assay.

In all hormone assays, the HRP-catalyzed color reaction was developed by incubation with a tetramethylbenzidine substrate solution. The enzyme-substrate reaction was terminated by a sulfuric acid stop solution, and the optical density was measured at 450 nm using a Chromate 4300 microplate reader (Awareness Technology Inc., Palm City, FL, US). The hormone concentrations in each sample were interpolated from their corresponding calibration curves plotted relating the intensity of the color to the concentration of calibrators.

2.9. Determination of testicular androgenic enzyme activities

Testicular activities of 3β-HSD and 17β-HSD were assessed according to the methods of Talalay (1962) and Jarabak et al. (1962), respectively. The assays were based on determining the rates of reduction in nicotinamide adenine dinucleotide (NAD^+) and nicotinamide adenine dinucleotide phosphate ($NADP^+$) in the presence of dehydroepiandrosterone and testosterone, respectively, by monitoring the increase in absorbance at 340 nm using a Jenway 6305 UV/Visible Spectrophotometer (Keison Products, Chelmsford, UK).

2.10. Determination of testicular oxidative stress markers

Testicular MDA concentrations were determined by the thiobarbituric acid assay (Uchiyama and Mihara, 1978). Testicular GPx activity was determined by monitoring the rate of glutathione (GSH) oxidation by hydrogen peroxide (H_2O_2) in the presence of NADPH, as measured by a decrease in absorbance at 340 nm (Paglia and Valentine, 1967). Testicular catalase activity was assayed by following the decrease in absorbance at 240 nm due to the decomposition of H_2O_2 (Aebi, 1984).

2.11. Determination of tissue protein content

Testicular tissue protein concentrations were determined using Folin-Ciocalteu reagent with bovine serum albumin as standard (Lowry et al., 1951).

2.12. Gene expression analyses

Total RNA was extracted from testicular tissues using the RNeasy Plus Mini kit (Qiagen, Venlo, The Netherlands), according to the manufacturer's instructions. The concentration of RNA was determined using the NanoDrop ND-1000 spectrophotometer (Thermo Fisher Scientific, Waltham, US) at 260 nm and its purity was assessed by the 260/280 nm absorbance ratio which ranged from 1.8 to 2.1. RNA integrity was confirmed by ethidium bromide-stain analysis of 28S and 18S bands by formaldehyde-containing agarose gel electrophoresis. An amount of 5 μg of the isolated total RNA was reverse-transcribed into complementary DNA (cDNA) using the RevertAid First Strand cDNA Synthesis Kit (MBI Fermentas, Hanover, US), employing a recombinant Moloney Murine Leukemia Virus (M-MuLV) reverse transcriptase reaction, according to the manufacturer's protocol.

To determine the testicular mRNA expression of StAR and c-kit, qRT-PCR was conducted in an optical 96-well reaction plate with an ABI PRISM Fast Sequence Detection System (Applied Biosystems, California, US), using SYBR Green PCR Master Mix (Applied Biosystems, California, US) and employing the following cycling conditions: 95 °C for 10 min, followed by 40 cycles of 95 °C for 15 s and 60 °C for 60 s. Glyceraldehyde-3-phosphate dehydrogenase (GAPDH)

Table 1
List of primer sequences used in real-time qPCR analysis.

Gene name	Primer sequence	Accession number	Tm (°C)	Product size (bp)
StAR	F: 5′-CACAGTCATCACCCATGAGC-3′	NM_031558.3	58.6	166
	R: 5′-AGCTCTGATGACACCGCTTT-3′		59.7	
c-kit	F: 5′-CTGGTGGTTCAGAGTTTCCATAGAC-3′	NM_022264.1	61.1	402
	R: 5′-TCAACGACCTTCCCGAAGG-3′		59.3	
GAPDH	F: 5′- TTGGTATCGTGGAAGGACTCA-3′	NM_017008.4	58.5	270
	R: 5′- TGTCATCATATTTGGCAGGTTT-3′		56.3	

StAR, steroidogenic acute regulatory protein; GAPDH, Glyceraldehyde-3-phosphate dehydrogenase.

was used as the housekeeping gene. The primer sequences used are shown in Table 1. Relative expression of the studied genes was calculated using the comparative cycle threshold method. All values were normalized to the GAPDH gene and expressed as fold change compared to the controls (Livak and Schmittgen, 2001).

2.13. Analysis of DNA damage via the comet assay

The comet assay was performed according to the method described by Singh et al. (1988), as modified by El-Kashlan et al. (2015). Briefly, cell suspensions prepared from testicular tissue were mixed with 1% low-melting-point agarose in PBS, and immediately spread on slides pre-coated with 0.8% agarose in PBS. After lysis in 0.045 M Tris-Borate-EDTA (TBE) buffer, pH 8.4, containing 2.5% sodium dodecyl sulfate (SDS), electrophoresis was conducted in an electrophoresis chamber containing the same TBE buffer, but devoid of SDS. The electrophoresis conditions were 2 V/cm for 2 min and 100 mA. Then, staining with 20 μg/mL ethidium bromide was performed at 4 °C. For visualization of DNA damage, ethidium bromide-stained DNA was examined using a fluorescent microscope (Olympus BX51, Tokyo, Japan). Quantification of DNA damage was performed by measuring the length of DNA migration and the percentage of migrated DNA using a Komet 5 image analysis software (Kinetic Imaging Ltd., Liverpool, UK) equipped with a charge-coupled device camera. The program also calculated the tail moment. The DNA fragment migration patterns of 50 to 100 randomly selected cells were analyzed per sample.

2.14. Statistical analysis

Data are expressed as mean ± S.D. All our data passed D'Agostino & Pearson omnibus, Shapiro-Wilk and/or Kolmogorov-Smirnov tests for normality. Comparisons were thus performed using one-way analysis of variance followed by Tukey's multiple comparison tests. The analysis was done using GraphPad Prism 6.01. *P*-values < .05 were considered statistically significant. In the figures and tables, a, b and c represent significant differences from control, SP and EMF groups, respectively. *, # and † denote statistical significance at $P < .001$, $P < .01$ and $P < .05$, respectively.

3. Results

3.1. Effect of exposure to EMF with or without spermine treatment on rat testicular histology and histomorphometric parameters

Control rats exhibited normal histological structure of seminiferous tubules with different stages of germinal epithelium cells and separated by interstitial cells of Leydig. Spermine-treated rats also displayed normally organized germinal epithelium. EMF-exposed rats showed sloughing and vacuolation of germinal epithelium, spermatid giant cells and congestion of intertubular blood vessels with edema. Rats in the EMF + SP group displayed restoration of germinal epithelium and interstitial tissue, with only mild vacuolation of the germinal epithelium (Fig. 1).

Testicular sections from EMF-exposed rats revealed significant 33.2%-decrease in seminiferous tubule epithelial height as compared to the controls. The effects of exposure to EMF were significantly abolished by spermine administration, resulting in 29.5% higher values in the EMF + SP in comparison to the EMF group. On the other hand, no significant differences were detected between the different studied groups regarding the seminiferous tubule diameter (Fig. 1). Furthermore, exposure to EMF resulted in significant 84.2% increase in STBM thickness as compared with the controls, an effect significantly abrogated by spermine treatment (42% lower values in the EMF + SP in comparison to the EMF group; Fig. 2).

3.2. Effects of exposure to EMF with or without spermine treatment on rat epididymal sperm profile

Rats exposed to EMF showed significant 41%, 49% and 30% reductions in sperm count, motility and live/dead ratio, respectively, as compared to the controls. Treatment with spermine significantly increased sperm count and motility restoring them back to normal and resulting in 61%, 83% and 35% higher sperm count, motility and live/dead ratio, respectively, compared to the corresponding values in the EMF-exposed rats. Moreover, EMF-exposed rats exhibited significant 2.2-fold increase in sperm abnormalities as compared to the controls. Treatment with spermine prevented these abnormalities, with levels significantly lower by 41.5% than those in the EMF group (Table 2).

3.3. Effects of exposure to EMF with or without spermine treatment on rat serum concentrations of inhibin B, activin A, gonadotrophins and steroid sex hormones

EMF-exposed rats exhibited significant 142.8%, 79.0% and 35.3% elevations in serum activin A, FSH and LH concentrations, respectively, as well as 48.5% and 60.4% declines in serum testosterone and inhibin B concentrations, respectively, in comparison to the controls. Additionally, exposure to EMF induced significant 3.1-fold elevation in serum estradiol concentration.

Spermine administration limited EMF-attributed alterations in the serum concentrations of testosterone, inhibin B, activin A, FSH and LH, resulting in 53% and 125% higher serum testosterone and inhibin B concentrations along with 38%, 30% and 17.4% lower activin A, FSH and LH concentrations, respectively, in the EMF + SP in comparison to the EMF group. Moreover, EMF + SP rats showed 44.7% significantly lower estradiol concentrations than EMF rats (Table 3).

3.4. Effects of exposure to EMF with or without spermine treatment on rat testicular steroidogenic and spermatogenic markers

Exposure to EMF led to significant 43.3% and 33.6% declines in testicular 3β-HSD and 17β-HSD activities, respectively, compared to the controls. Spermine treatment significantly raised the enzyme activities by 33.7% and 21.8%, respectively, relative to the corresponding activities in the EMF group. Moreover, rats exposed to EMF showed significant 58.7% and 37.7% reductions in testicular StAR and c-kit mRNA expression compared to the controls. By contrast, their spermine-treated counterparts showed significantly improved values that

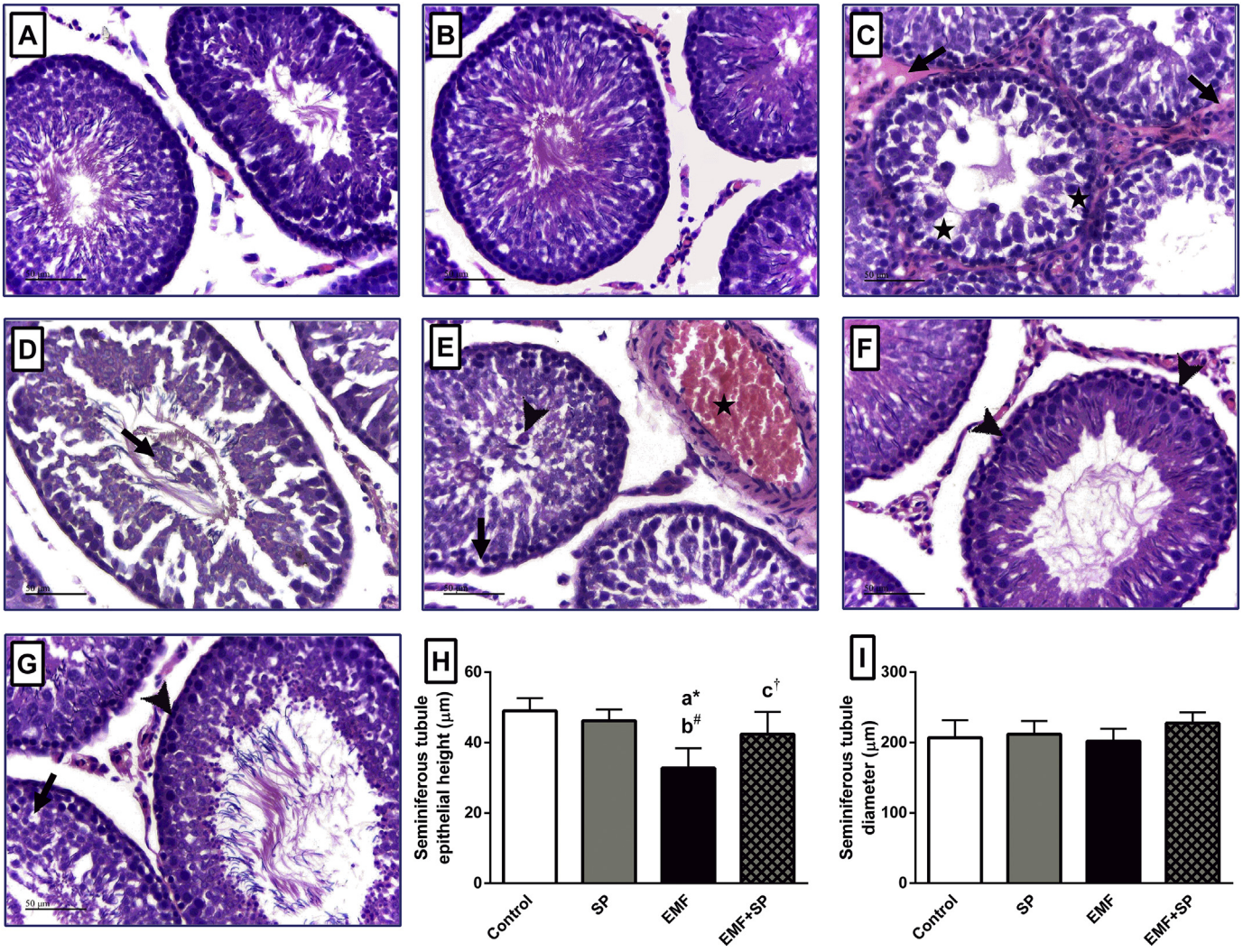


Fig. 1. Effects of the exposure to electromagnetic field (EMF) with and without spermine (SP) treatment on testicular histology, seminiferous tubule epithelial height and seminiferous tubule diameter in rats: (A-G) Histological assessment of testicular tissues using H&E stain (X400). Control group demonstrating normal histological structure of seminiferous tubule with different stages of germinal epithelium cells and separated by interstitial cells of Leydig (Panel A). SP group showing apparently normally organized germinal epithelium with mild vacuolation (Panel B). EMF group showing vacuolation of germinal epithelium (stars), absence of spermatids with a relative decrease in spermatocytes and intertubular edema (arrows; Panel C). EMF group showing premature sloughing of germinal epithelium (arrow; Panel D). EMF group showing vacuolation of germinal epithelium (arrow), start of formation of spermatid giant cells (arrow head) and severe congestion of intertubular blood vessels (star; Panel E). EMF + SP group showing apparently normal seminiferous tubules with mild vacuolation of germinal epithelium (arrows), more prominent spermatogonial cells (arrow heads) and presence of spermatid stages (Panels F & G). Seminiferous tubule epithelial height and seminiferous tubule diameter, respectively, expressed as mean ± S.D. of 6 rats (Panels H & I). a, b and c represent significant differences from control, SP and EMF groups, respectively. *, # and † denote statistical significance at $P < .001$, $P < .01$ and $P < .05$, respectively (one-way ANOVA with subsequent Tukey's multiple comparisons test).

were 180% and 46% higher than in the EMF group, respectively (Fig. 3).

3.5. Effects of exposure to EMF with or without spermine treatment on rat testicular oxidative stress markers

EMF-exposed rats exhibited significant 2.83-fold increase in testicular level of MDA, the index of lipid peroxidation, relative to the controls. This effect was significantly alleviated by spermine treatment which led to 33.8% lower MDA content when comparing the EMF + SP and EMF groups.

Exposure to EMF caused significant 50% decrease in testicular catalase activity. Treatment with spermine resulted in significant 2.2-fold elevation in catalase activity when comparing the EMF + SP and EMF groups, thereby preventing its deterioration.

Rats in the EMF group displayed significant 81.6% drop in testicular GPx activity when compared with the controls. On the other hand, significant 8.1-fold elevation in GPx activity was noted in the EMF + SP group when compared with the EMF group. The EMF + SP group showed significantly 49%-higher activity in comparison to the control group (Table 4).

3.6. Effects of exposure to EMF with or without spermine treatment on rat testicular apoptosis

Exposure to EMF caused dramatic increase in testicular caspase-3 expression, as manifested by almost 11.5-fold increase in caspase-3 immunostained area percentage when compared with the control. Such intense apoptotic status was markedly attenuated by treatment with spermine which resulted in 54.5% lower immunohistochemically detected caspase-3 expression than in the EMF-exposed rats (Fig. 4).

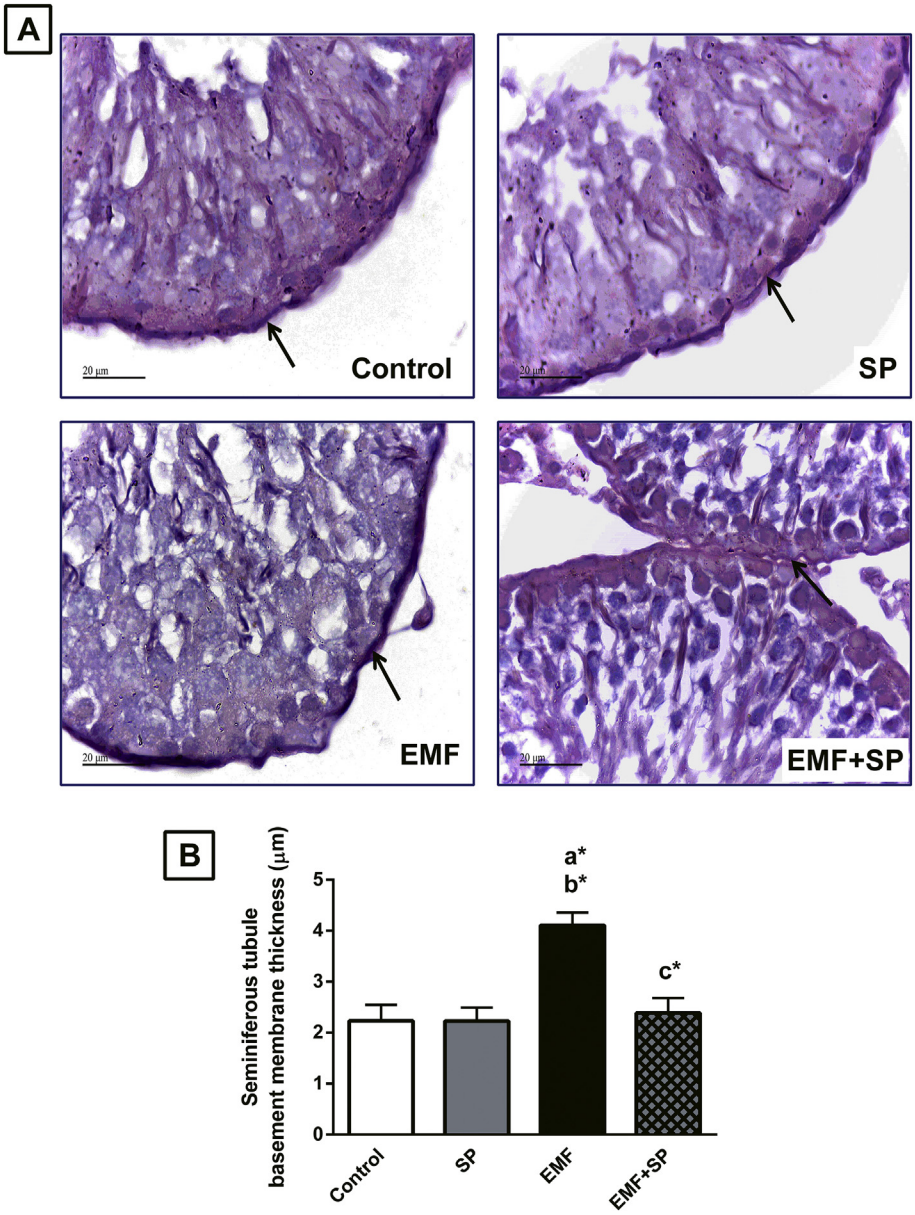


Fig. 2. Effects of the exposure to electromagnetic field (EMF) with and without spermine (SP) treatment on seminiferous tubule basement membrane thickness in rats. Representative photomicrographs of periodic acid Schiff (PAS)-stained sections in the testes of rats from the different studied groups (arrow; X1000; Panel A). Seminiferous tubule basement membrane thickness expressed as mean ± S.D. of 6 rats (Panel B). a, b and c represent significant differences from control, SP and EMF groups, respectively. * denotes statistical significance at $P < .001$ (one-way ANOVA with subsequent Tukey's multiple comparisons test).

3.7. Effects of exposure to EMF with or without spermine treatment on rat testicular DNA damage

Comet assay revealed noticeable DNA damage in the testicular tissue of EMF-exposed rats as evidenced by 6.6-fold increase in tailed percentage, 2.2-fold increase in tail length and tail DNA, and 5.4-fold increase in tail moment, relative to the controls. Spermine administration significantly decreased the tailed percentage by 21.2%, tail DNA by 13.8% and tail moment by 20%, but non-significantly reduced the tail length by 7.1% compared to the EMF-exposed rats (Fig. 5).

Table 2
Effects of the exposure to electromagnetic field (EMF) with and without spermine (SP) treatment on epididymal sperm count, motility, viability and morphology in the rat.

	Control	SP	EMF	EMF + SP
Count (millions/mL)	207.5 ± 59.31	217.5 ± 54.64	122.5 ± 35.74 $^{a\dagger b\#}$	197.5 ± 51.88 ^{c†}
Motility (%)	70.0 ± 16.32	74.0 ± 17.43	36.0 ± 5.66 $^{a_* b_*}$	66.0 ± 17.27 $^{c\#}$
Live/dead sperm ratio (%)	73.3 ± 24.94	77.5 ± 7.07	51.0 ± 6.93 $^{a\dagger b\dagger}$	69.0 ± 12.15
Sperm abnormality (%)	23.0 ± 6.24	21.7 ± 7.25	49.8 ± 11.37 $^{a_* b_*}$	29.1 ± 10.06 ^{c_*}

Values represent mean ± S.D. of 8 rats. a, b and c represent significant differences from control, SP and EMF groups, respectively. *, # and † denote statistical significance at $P < .001$, $P < .01$ and $P < .05$, respectively (One-way ANOVA followed by Tukey's multiple comparisons test).

Table 3
Effects of the exposure to electromagnetic field (EMF) with and without spermine (SP) on the serum inhibin B, activin A, follicle stimulating hormone (FSH), luteinizing hormone (LH), testosterone (T) and estradiol (E2) concentrations in the rat.

	Control	SP	EMF	EMF + SP
Inhibin B (pg/mL)	158.4 ± 14.37	156.9 ± 12.91	62.7 ± 12.6 ^{a_*b_*}	141.0 ± 16.21 ^{c_*}
Activin A (pg/mL)	267.0 ± 27.61	270.3 ± 31.63	648.4 ± 38.74 ^{a_*b_*}	402.6 ± 43.76 ^{a_*b_*c_*}
FSH (ng/mL)	5.2 ± 1.44	4.9 ± 1.21	9.3 ± 2.06 ^{a_*b_*}	6.5 ± 1.76 ^{c†}
LH (ng/mL)	1.7 ± 0.34	1.6 ± 0.37	2.3 ± 0.14 ^{a_*b_*}	1.9 ± 0.23 ^{c†}
T (ng/mL)	3.3 ± 0.65	3.2 ± 0.65	1.7 ± 0.37 ^{a_*b_*}	2.6 ± 0.44 ^{c†}
E2 (pg/mL)	40.1 ± 12.09	37.0 ± 8.68	123.9 ± 14.21 ^{a_*b_*}	68.5 ± 13.64 ^{a_*b_*c_*}

Values represent mean ± S.D. of 8 rats. a, b and c represent significant differences from control, SP and EMF groups, respectively. *, # and † denote statistical significance at $P < .001$, $P < .01$ and $P < .05$, respectively (One-way ANOVA followed by Tukey's multiple comparisons test).

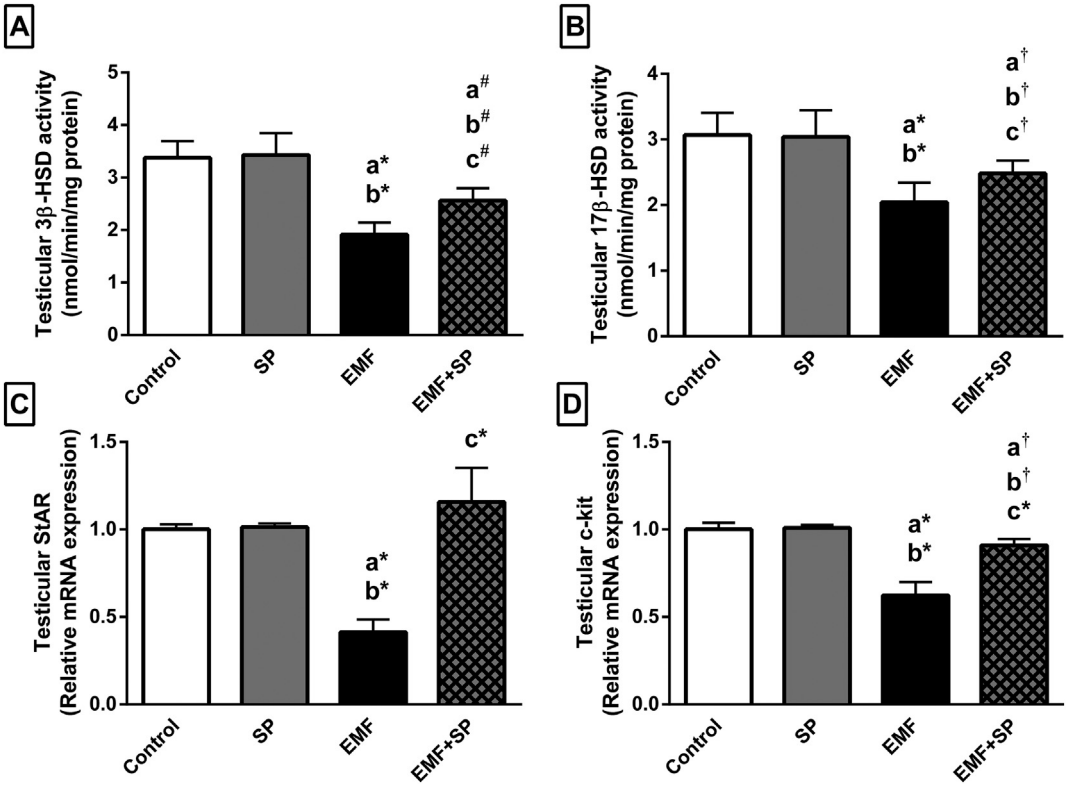


Fig. 3. Effects of the exposure to electromagnetic field (EMF) with and without spermine (SP) treatment on testicular steroidogenic and spermatogenic markers in rats: Testicular activities of 3β-hydroxysteroid dehydrogenase, 3β-HSD (Panel A) and 17β-hydroxysteroid dehydrogenase, 17β-HSD (Panel B) and relative mRNA expression of testicular steroidogenic acute regulatory protein, StAR (Panel C) and c-kit (Panel D). Data are expressed as mean ± S.D. (Panels A & B) and mean fold change ± S.D. (Panels C & D) of 6 rats. a, b and c represent significant differences from control, SP and EMF groups, respectively. *, # and † denote statistical significance at $P < .001$, $P < .01$ and $P < .05$, respectively (one-way ANOVA with subsequent Tukey's multiple comparisons test).

Table 4
Effects of the exposure to electromagnetic field (EMF) with and without spermine (SP) on the testicular malondialdehyde (MDA) concentration and catalase (CAT) and glutathione peroxidase (GPx) activities in the rat.

	Control	SP	EMF	EMF + SP
MDA (nmol/g tissue)	7.50 ± 1.95	7.41 ± 1.95	21.25 ± 3.59 ^{a_*b_*}	14.06 ± 2.09 ^{a_*b_*c_*}
CAT (U/mg protein)	0.70 ± 0.13	0.68 ± 0.14	0.35 ± 0.09 ^{a_*b_*}	0.76 ± 0.20 ^{c_*}
GPx (U/mg protein)	0.049 ± 0.012	0.051 ± 0.011	0.009 ± 0.003 ^{a_*b_*}	0.073 ± 0.017 $^{a\#b\#c_*}$

Values represent mean ± S.D. of 8 rats. a, b and c represent significant differences from control, SP and EMF groups, respectively. * and # denote statistical significance at $P < .001$ and $P < .01$, respectively (One-way ANOVA followed by Tukey's multiple comparisons test).

3.8. Effects of exposure to EMF with or without spermine treatment on rat testicular inflammatory markers

Immunohistochemical staining of testicular tissue from EMF-exposed rats revealed substantial expression of NF-κB p65, iNOS and COX-2, relative to control rats. Considerable decline in these expressions was observed in spermine-treated EMF-exposed rats, as manifested by 74%, 56.7% and 56.4% lower NF-κB p65, iNOS and COX-2 immunostained area percentages, respectively, when compared to the EMF group rats (Figs. 6–8).

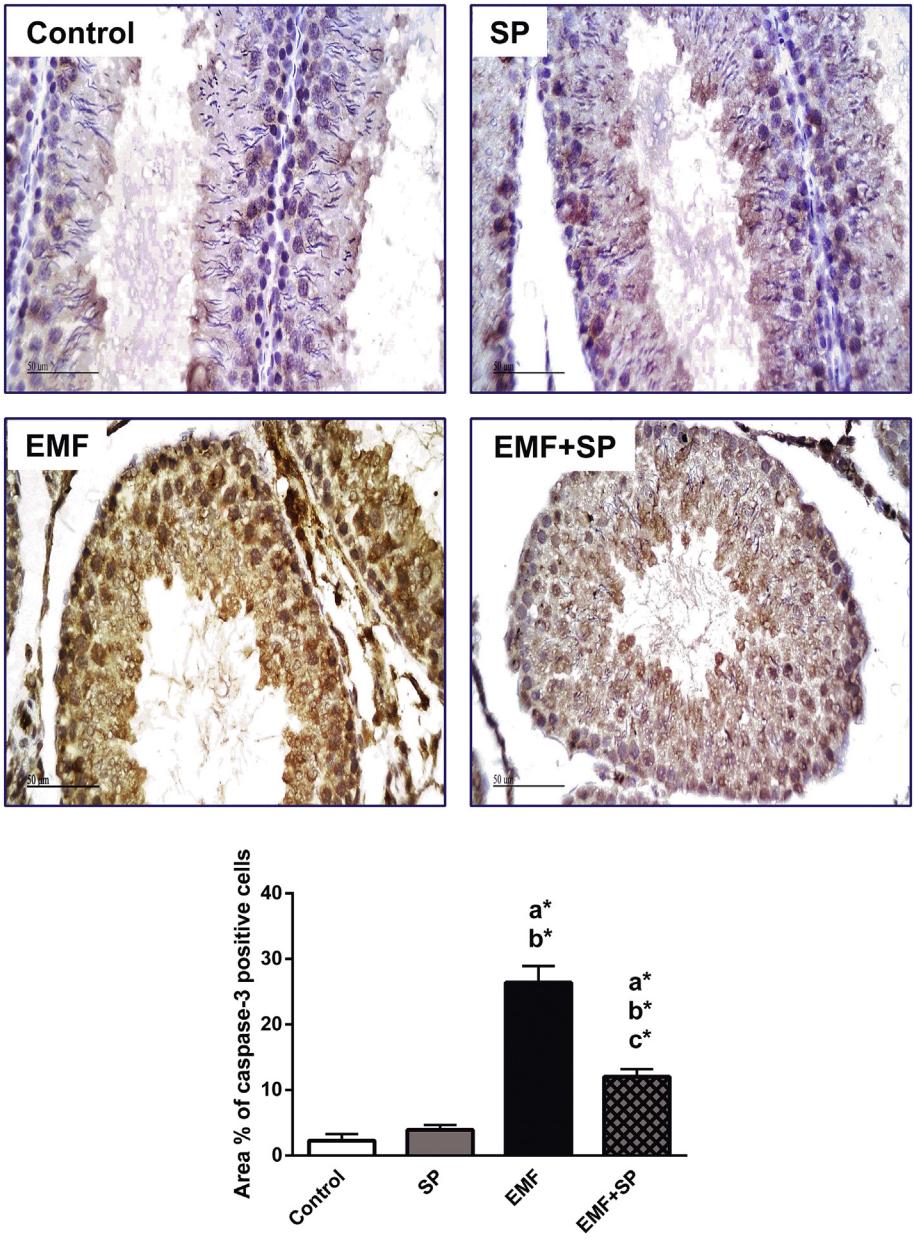


Fig. 4. Effects of the exposure to electromagnetic field (EMF) with and without spermine (SP) treatment on testicular apoptosis in rats: Immunohistochemical staining of caspase-3 and quantification of staining as area percentage of immunopositive cells to the total area of microscopic field across 6 fields (X400). Data are expressed as mean ± S.D. of 6 rats. a, b and c represent significant differences from control, SP and EMF groups, respectively. * denotes statistical significance at $P < .001$ (one-way ANOVA with subsequent Tukey's multiple comparisons test).

4. Discussion

To date, increasing exposure to EMF raises multiple concerns since technologies extensively employing portable communication systems have become omnipresent. Our investigations clearly demonstrated the adverse effects of EMF exposure on male rat fertility and the protective potential of spermine against EMF-induced testicular and reproductive aberrations.

When analyzing testis histology, seminiferous tubule epithelial height represents an index of normal epithelial cell architecture with harmonic germinal cell associations. EMF-induced decrease in epithelial height we observed, indicates defective cell connections in the germ epithelium, possibly attributed to the observed cell sloughing in testes (Damodar et al., 2012). Our observed decrease in germinal epithelial height as well as the histologically observed vacuolation and absence of spermatids are in line with Hancı et al. (2018). However, in contrast to our findings, these authors reported a decrease in the STD. STBM plays a distinct role in spermatogenesis, serving as proliferation site for spermatogonia, a support for the phenotypic differentiation of Sertoli cells and for maintaining the immunological function of the seminiferous epithelium. Ultrastructural anomalies in STBM are assumed to cause infertility (Kahsai et al., 1997). Therefore, the defective sperm profile in the EMF-exposed rats could be related to the abnormally thickened STBM, an assumption supported by the amended sperm parameters associating restored STBM thickness in the spermine-treated group. Sufficient testosterone levels are crucial for maintaining structural morphology and physiology of the seminiferous tubules and for proper functioning of the seminiferous epithelium (Holdcraft and Braun, 2004). Thus, the morphometric alterations resulting from EMF exposure and their effective prevention by spermine may be explained, at least in part, by the changes in testosterone.

The disrupted sperm count, viability, motility and morphology

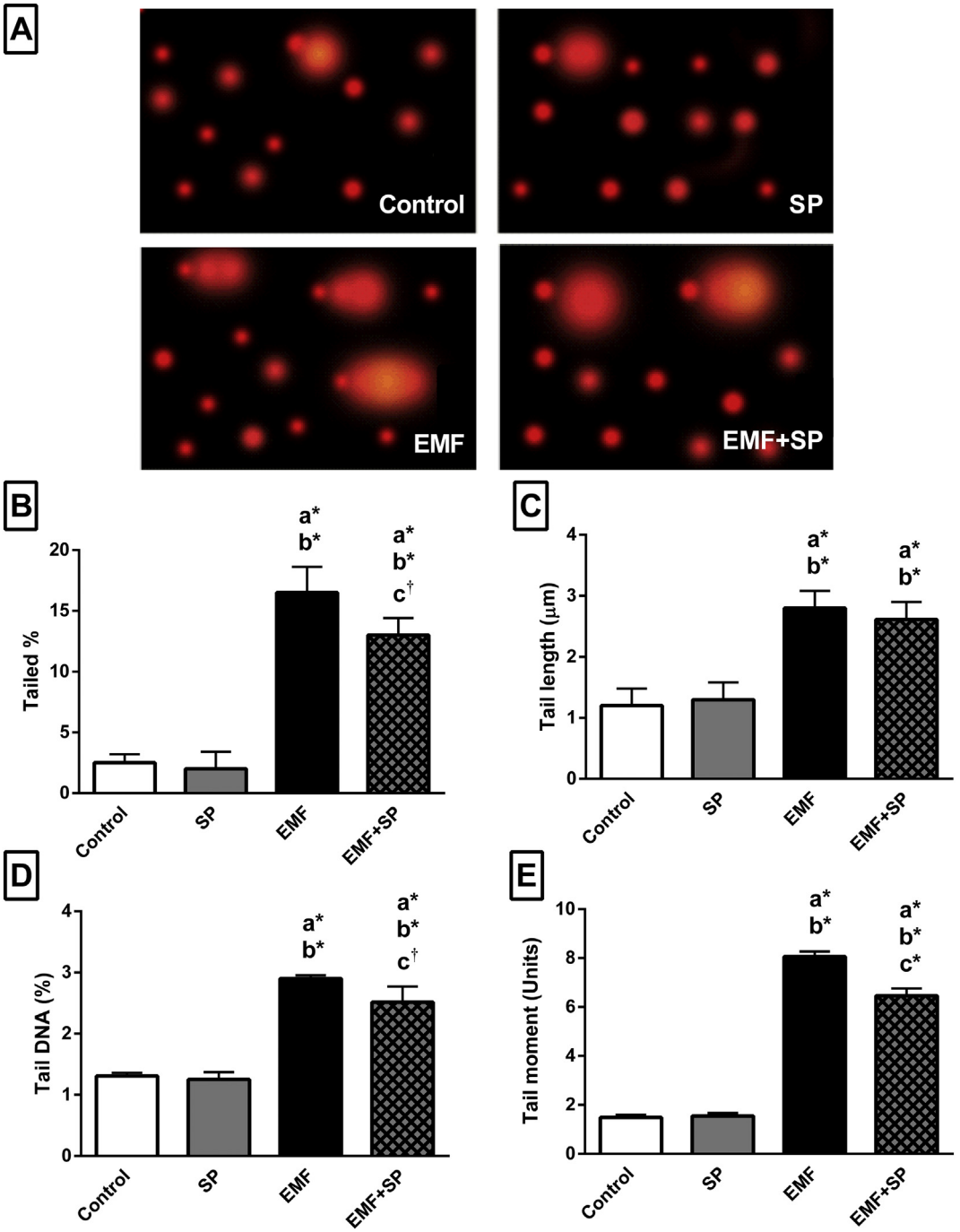


Fig. 5. Effects of the exposure to electromagnetic field (EMF) with and without spermine (SP) treatment on testicular DNA damage in rats: Representative photographs of testicular cells analyzed by the comet assay for quantification of DNA damage (X40; Panel A); tailed percentage (Panel B); tail length (Panel C); tail DNA (Panel D) and tail moment (Panel E). Data are expressed as mean ± S.D. of 6 rats. a, b and c represent significant differences from control, SP and EMF groups, respectively. * and † denote statistical significance at $P < .001$ and $P < .05$, respectively (one-way ANOVA with subsequent Tukey's multiple comparisons test).

observed in EMF-exposed rats in our study are consistent with Agarwal et al. (2008). The deranged sperm parameters may be explained in light of the observed oxidative, apoptotic and DNA perturbations. Rat exposure to EMF for 2 h/day for 35 days has been reported to cause elevation in semen ROS and sperm MDA levels along with decline in sperm GPx activity (Kesari et al., 2011). The mitochondria have been implicated as significant source of ROS in the male reproductive system under EMF exposure (Santini et al., 2018). The high content of polyunsaturated fatty acids in the plasma membrane and the relative scarcity of ROS scavenging enzymes, owing to the virtual absence of cytoplasm, render mature spermatozoa vulnerable to ROS attack resulting in lipid peroxidation (Opuwari and Henkel, 2016). Lipid peroxidation increases membrane permeability, diminishes motility and causes aberrations that weaken the fertilizing capacity in mammalian spermatozoa (Rao et al., 1989). Distortions in sperm head and midpiece were formerly reported in radiofrequency-exposed rats, ascribed to the excessive ROS generation (Kesari et al., 2011) inducing sperm apoptosis through enhancing sperm caspase-3 activity (Kesari and Behari, 2012). ROS adversely alter the biofunctional sperm profile, increasing spermatozoa with fragmented DNA and inversely correlating with sperm count, motility, morphology and fertilization rate (Ding et al., 2018; Opuwari and Henkel, 2016). Thus, enhanced DNA fragmentation

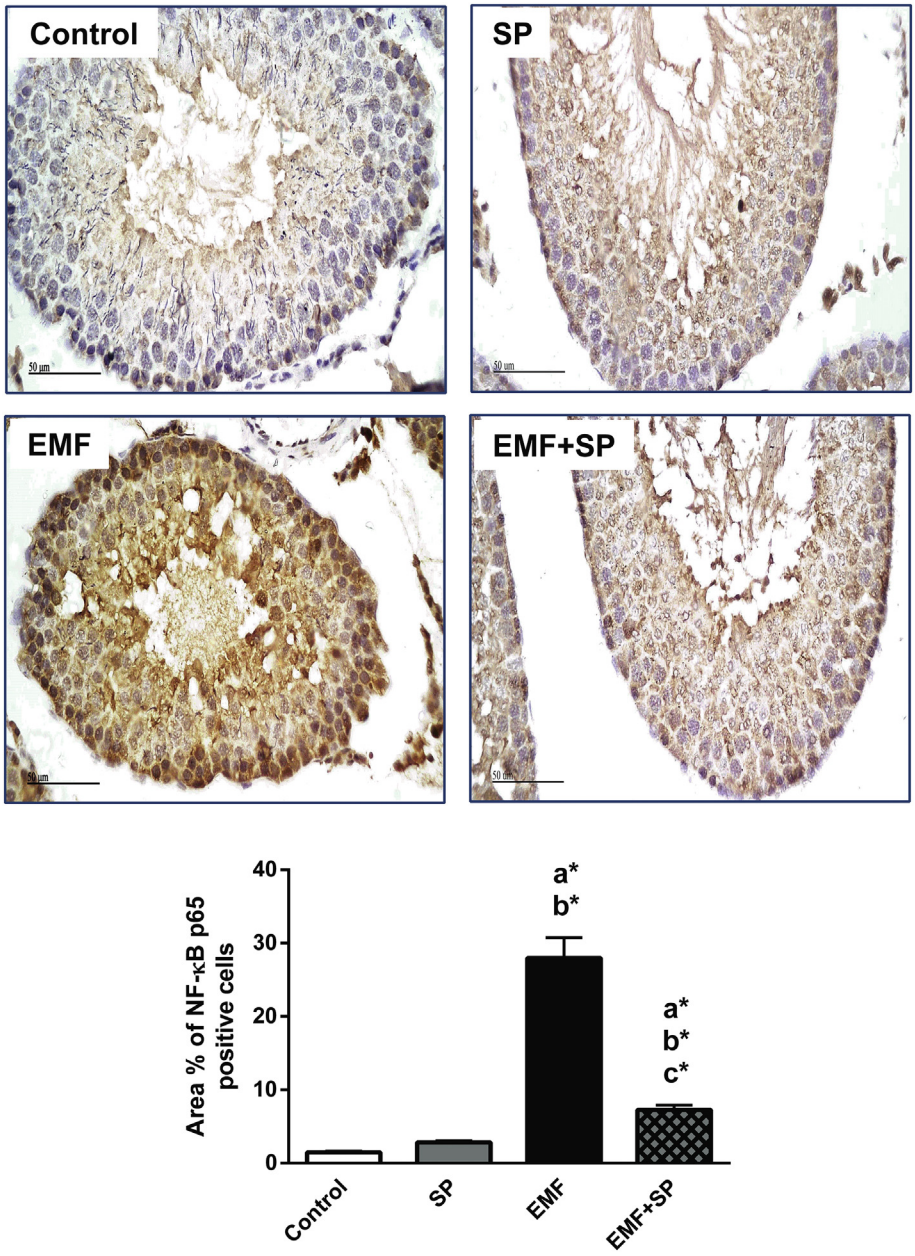


Fig. 6. Effects of the exposure to electromagnetic field (EMF) with and without spermine (SP) treatment on testicular expression of nuclear factor kappa B p65 (NF-κB p65) in rats: Immunohistochemical staining of NF-κB p65 and quantification of staining as area percentage of immunopositive cells to the total area of microscopic field across 6 fields (X400). Data are expressed as mean ± S.D. of 6 rats. a, b and c represent significant differences from control, SP and EMF groups, respectively. * denotes statistical significance at $P < .001$ (one-way ANOVA with subsequent Tukey's multiple comparisons test).

contributes to the impaired sperm profile. Noteworthy, human spermatozoa exposure to EMF in the radiofrequency range and power density of mobile phones instigated mitochondrial ROS generation and enhanced DNA base adduct formation and eventually DNA fragmentation (Odacı and Özyılmaz, 2015).

Compelling literature supports a vital role of polyamines in testicular development and spermatogenesis. Ornithine-decarboxylase-1 (ODC1), the rate-limiting enzyme of polyamine biosynthesis, exhibits stage- and cell-specific expression in rodent testis during spermatogenesis showing considerable elevation during the first spermatogenic wave (Alcivar et al., 1989; Kaipia et al., 1990). Spermine is essential for the spermatogenesis completion since transgenic mice with an inactivating mutation of spermine synthase exhibit infertility and arrested spermatogenesis at the spermatogonia and primary spermatocyte stages (Wang et al., 2004). Mechanisms underlying the ameliorative effect of polyamines on sperm motility are not fully elucidated, but *in vitro* studies provide explanations linked to intracellular signaling and sperm energy metabolism. Spermine enhances glycolysis in rat epididymal spermatozoa (Pulkkinen et al., 1975), stimulates adenylate cyclase activity and decreases the activity of phosphodiesterase, an inhibitor of cyclic-adenosine monophosphate signaling in human spermatozoa (Shah et al., 1975).

Our findings depict a notably altered serum hormone profile in the EMF-exposed rats. Similar pattern of decline in serum inhibin B and testosterone along with elevation in FSH and LH was reported upon long-term male rat exposure to EMF (Odacı and Özyılmaz, 2015). The markedly reduced testosterone in EMF-exposed rats is obviously the result of, firstly, their down-regulated testicular StAR, which mediates the rate-limiting step in steroidogenesis, and, secondly, their lowered testicular activities of 3β-HSD and 17β-HSD, the key-enzymes in

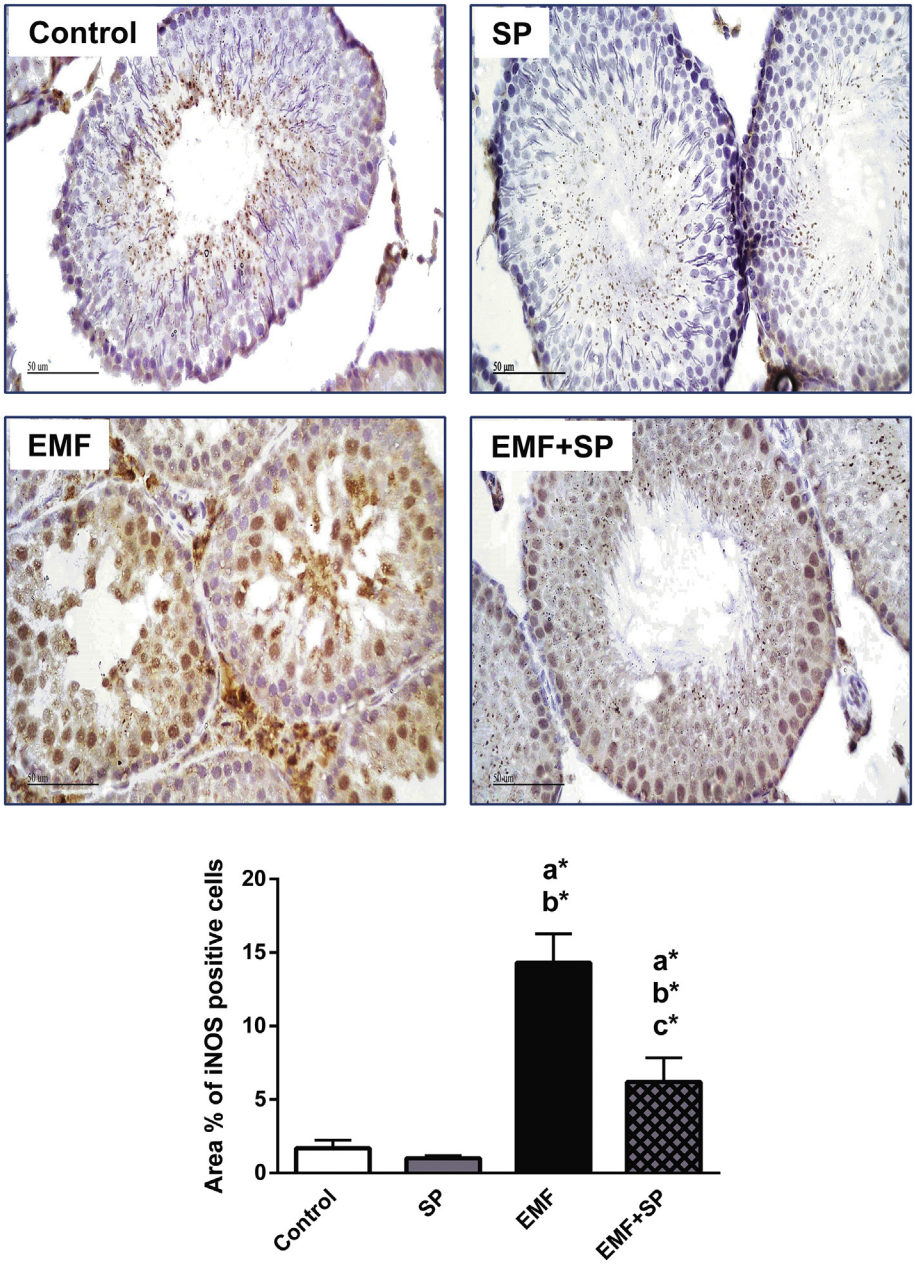


Fig. 7. Effects of the exposure to electromagnetic field (EMF) with and without spermine (SP) treatment on testicular expression of inducible nitric oxide synthase (iNOS) in rats: Immunohistochemical staining of iNOS and quantification of staining as area percentage of immunopositive cells to the total area of microscopic field across 6 fields (X400). Data are expressed as mean ± S.D. of 6 rats. a, b and c represent significant differences from control, SP and EMF groups, respectively. * denotes statistical significance at $P < .001$ (one-way ANOVA with subsequent Tukey's multiple comparisons test).

testicular androgenesis. Noteworthy, activated NF-κB has been reported to down-regulate steroidogenic enzyme gene expression in Leydig cells (Hong et al., 2004), lending support to the currently observed pattern of alterations in NF-κB p65, StAR, 3β-HSD, 17β-HSD and testosterone. Ability of spermine to boost steroidogenesis and to reinstate the testosterone level could be attributed to its ability to hamper EMF-induced NF-κB activation. The restoration of normal testosterone level achieved by spermine is consistent with the role of polyamines in steroidogenesis, as demonstrated by steroid synthesis reduction in rodent testis after ODC1 inhibition (Mäkitie et al., 2009).

Elevation in serum FSH in EMF-exposed rats is considered as an endocrine index of germinal epithelial damage (Bergmann et al., 1994), consistent with our histomorphometric observations. The observed elevations in serum LH and FSH in EMF-exposed rats are in accordance with former reports (Sepehrimanesh et al., 2014b) and could result from a feedback mechanism in response to the notable decline in testosterone (Shahin and Mohamed, 2017). Another important feedback signal for FSH production is the Sertoli cell hormone, inhibin B, which showed significantly decreased serum levels in EMF-exposed rats, thereby providing another explanation for the elevated serum FSH. As important endocrine marker of spermatogenesis (Foppiani et al., 1999), inhibin B decline indicates impaired spermatogenesis in parallel with the decline in sperm parameters and testicular c-kit expression. Alterations in serum FSH level are also in accordance with the corresponding activin A changes. The observed activation of NF-κB in EMF-exposed rats could contribute to their elevated activin A level *via* activation of mitogen activated protein kinases and subsequent production of the transcription factor AP-1. The activin β_A subunit promoter contains multiple AP-1 responsive elements (Ardekani et al., 1998; Tanimoto et al., 1996), indicating that the stimulation of activin A

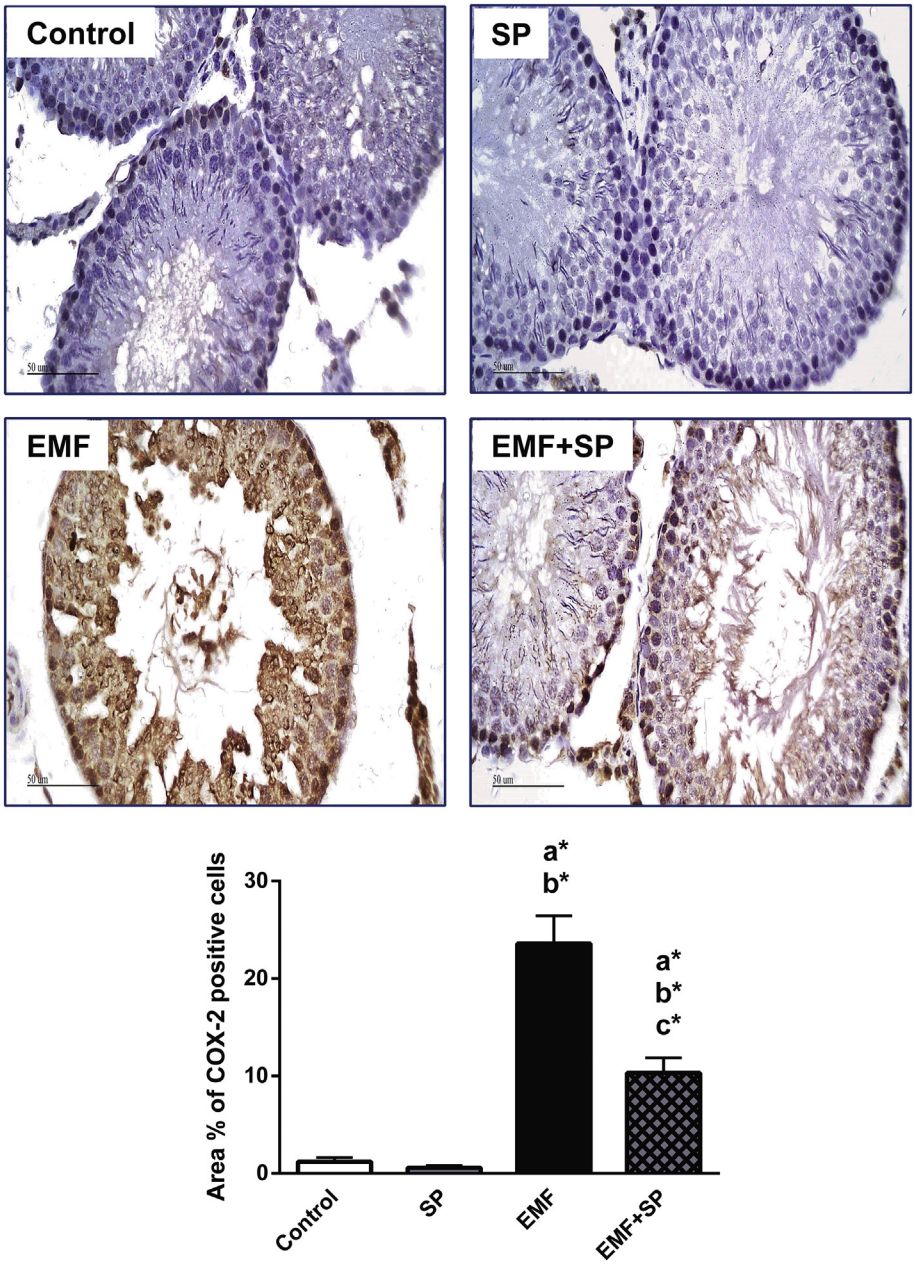


Fig. 8. Effects of the exposure to electromagnetic field (EMF) with and without spermine (SP) treatment on testicular expression of cyclooxygenase-2 (COX-2) in rats: Immunohistochemical staining of COX-2 and quantification of staining as area percentage of immunopositive cells to the total area of microscopic field across 6 fields (X400). Data are expressed as mean ± S.D. of 6 rats. a, b and c represent significant differences from control, SP and EMF groups, respectively. * denotes statistical significance at $P < .001$ (one-way ANOVA with subsequent Tukey's multiple comparisons test).

synthesis by inflammatory signaling involves this transcription factor (Okuma et al., 2005).

As marker for differentiating spermatogonia (Schrans-Stassen et al., 1999), c-kit down-regulation in the testicular tissue of EMF-exposed rats may indicate spermatogenesis disruption, as manifested by the observed perturbations in sperm count, viability, motility and morphology. Decline in c-kit mRNA level along with impaired spermatogenesis are consistent with earlier reports (Shahin and Mohamed, 2017). The benefit of spermine against EMF-associated defective spermatogenesis is obviously revealed by the markedly up-regulated c-kit gene expression level.

In our study, exposure to EMF resulted in deranged testicular oxidative status, manifested by the significant increase in the lipid peroxidation marker, MDA, and decrease in the antioxidant catalase and GPx activities. Enhanced testicular lipid peroxidation following exposure to 900 MHz EMF is in accordance with Hancı et al. (2018). However, contradictory to our findings, they reported an increase in catalase activity. In particular, GPx is the chief enzyme responsible for H_2O_2 elimination in the testis (Peltola et al., 1992). Therefore, its reduced activity may ultimately lead to imbalanced GSSG/GSH redox couple and hence predispose testicular tissue and sperms to H_2O_2-induced damage. Mitigation of EMF-induced oxidative aberrations with spermine supported its marked antioxidant capacity. Likewise, polyamines act as reactive oxygen species (ROS) scavengers (Ha et al., 1998) and mediate antioxidative defense by up-regulating antioxidant protein expression (Krüger et al., 2013).

EMF-induced impairment in oxidative status could greatly contribute to the immunohistochemically revealed increase in testicular expression of caspase-3, the key-apoptosis executioner. This notion could be justified by the expected accumulation of H_2O_2 as a

consequence of the reduced GPx and catalase activities, and is corroborated by the reported increase in caspase-3 activity in H_2O_2-treated testicular germ cells (Maheshwari et al., 2009). Instigation of germinal epithelial apoptosis in rats exposed to 900 MHz EMF has been lately reported (Hancı et al., 2018). Our findings revealed notable anti-apoptotic effects of spermine, obviously due to its potent antioxidant capacity, verified by the significant lowering in EMF-induced enhancement in testicular caspase-3 expression. Spermine has shown anti-apoptotic potential against lead and γ-irradiation-induced hepatotoxicity (Abu-Khudir et al., 2017). The observed protective effects of spermine against apoptosis are consistent with its reported ability to reduce ROS production and prevent apoptosis through increasing Bcl-2 expression and decreasing Bax expression, during canine sperm cryopreservation (Setyawan et al., 2016). In context, a former study reported enhanced susceptibility to apoptosis under conditions of polyamine depletion in intestinal epithelial cells (Li et al., 2001).

Our comet assays revealed testicular DNA fragmentation in EMF-exposed rats, significantly attenuated by spermine. ROS overproduction results in higher frequency of single- and double-strand DNA breaks and DNA/protein cross-linking (La Vignera et al., 2013). In a recent study on men exposed to electromagnetic radiation from 4G smartphone and 2.45-GHz Wi-Fi, comet assay of their semen revealed significant sperm DNA fragmentation (Ding et al., 2018). In line with the presently observed spermine-related improvement in DNA damage, protective effects of polyamines against radiation-induced DNA strand breaks (Spotheim-Maurizot et al., 1995), crosslinks to proteins (Chiu and Oleinick, 1998), and base degradation (Douki et al., 2000) have been reported. Several mechanisms have been suggested to explain the radioprotection conferred by polyamines including singlet oxygen quenching (Khan et al., 1992), hydroxyl radical scavenging (Spotheim-Maurizot et al., 1995) and DNA helix compaction into tightly packaged structures, thereby reducing DNA accessibility to hydroxyl radicals (Douki et al., 2000; Spotheim-Maurizot et al., 1995).

Exposure to EMF resulted in significant testicular NF-κB activation, possibly explained by EMF-related alterations in the activities of protein kinase C and protein tyrosine kinases (Uckun et al., 1995; Holian et al., 1996) which, in turn, play key-roles in NF-κB regulation (Baldwin, 1996; Imbert et al., 1996). In context, NF-κB activation was observed *in vitro* in mouse spermatogenic cell lines 48 h following EMF exposure (Solek et al., 2017). As a transcriptional activator of various inflammatory genes, activated NF-κB may explain the immunohistochemically detected overexpression of COX-2 and iNOS. The concurrently triggered NF-κB activation and inflammation in parallel with oxidative stress are in line with a recent report relating these events to the enhanced production of oxidants, including hydroxyl and NO_2 radicals, following EMF exposure (Pall, 2018). Additional major cellular protective systems can also be altered in EMF-exposed testis. In a rat model of human cell phone exposure, EMF was shown to alter the expression of heat shock proteins and chaperon molecules possibly contributing to non-thermal stress in the testicular tissue (Sepehrimanesh et al., 2017). Interestingly, up-regulation of ATP synthase B-subunit and hypoxia up-regulated protein-1 precursor affecting signaling pathways in rat testes and spermatogenesis and playing a critical role in protein folding and secretion in the endoplasmic reticulum were described (Sepehrimanesh et al., 2017). These alterations clearly contribute to the EMF-induced reproductive damage and generate possible carcinogenic risk. Our work illustrates the potent anti-inflammatory effect of spermine against EMF-induced testicular aberrations, as verified by its notable inhibitory effects on NF-κB activation and COX-2 and iNOS expression and supported by reports of induction of NF-κB activation and COX-2 up-regulation following polyamine depletion (Li et al., 2001; Parker and Gerner, 2002). The inhibitory effect of spermine on iNOS expression was formerly described (Blachier et al., 1997).

In conclusion, our study highlights the hazardous impact of EMF exposure on male rat fertility, as manifested by the impaired spermatogenesis and steroidogenesis with disrupted sperm and hormone profiles. Our study supports the potent protective contribution of spermine against EMF-induced aberrations, mediated, at least in part, by limiting EMF-induced oxidative, inflammatory, apoptotic and DNA perturbations.

Supplementary data to this article can be found online at https://doi.org/10.1016/j.taap.2019.03.009.

Conflict of interest

The authors declare that they have no conflict of interest.

Funding

This research did not receive any specific grant from any funding agency in the public, commercial or not-for-profit sector.

Acknowledgement

The authors gratefully acknowledge Dr. Mohamed Abdelrazek, Department of Pathology, Cairo University, Cairo, Egypt, for his valuable assistance in performing and analyzing the results of histological, histomorphometric and immunohistochemical examinations.

References

Abu-Khudir, R., Habieb, M.E., Mohamed, M.A., Hawas, A.M., Mohamed, T.M., 2017. Anti-apoptotic role of spermine against lead and/or gamma irradiation-induced hepatotoxicity in male rats. Environ. Sci. Pollut. Res. 24, 24272–24283. https://doi.org/10.1007/s11356-017-0069-0.

Aebi, H., 1984. Catalase in vitro. Methods Enzymol. 105, 121–126.

Agarwal, A., Deepinder, F., Sharma, R.K., Ranga, G., Li, J., 2008. Effect of cell phone usage on semen analysis in men attending infertility clinic: an observational study. Fertil. Steril. 89, 124–128. https://doi.org/10.1016/j.fertnstert.2007.01.166.

Alcivar, A.A., Hake, L.E., Mali, P., Kaipia, A., Parvinen, M., Hecht, N.B., 1989. Developmental and differential expression of the ornithine decarboxylase gene in rodent testis. Biol. Reprod. 41, 1133–1142.

Ardekani, A.M., Romanelli, J.C.D., Mayo, K.E., 1998. Structure of the rat inhibin and activin β_A -subunit gene and regulation in an ovarian granulosa cell line [1]. Endocrinology 139, 3271–3279. https://doi.org/10.1210/endo.139.7.6116.

Baldwin, A.S., 1996. The NF-kappa B and I kappa B proteins: new discoveries and insights. Annu. Rev. Immunol. 14, 649–683. https://doi.org/10.1146/annurev.immunol.14.1.649.

Bancroft, J.D., Gamble, M., 2008. Theory and Practice of Histological Techniques, Sixth. ed. Churchill Livingstone, Edinburgh.

Bergmann, M., Behre, H.M., Nieschlag, E., 1994. Serum FSH and testicular morphology in male infertility. Clin. Endocrinol. 40, 133–136.

Bilgici, B., Gun, S., Avci, B., Akar, A.K., Engiz, B., 2018. What is adverse effect of wireless local area network, using 2.45 GHz, on the reproductive system? Int. J. Radiat. Biol. 94, 1054–1061. https://doi.org/10.1080/09553002.2018.1503430.

Blachier, F., Mignon, A., Soubrane, O., 1997. Polyamines inhibit lipopolysaccharide-induced nitric oxide synthase activity in rat liver cytosol. Nitric Oxide 1, 268–272. https://doi.org/10.1006/NIOX.1997.0127.

Chiu, S., Oleinick, N.L., 1998. Radioprotection of cellular chromatin by the polyamines spermine and putrescine: preferential action against formation of DNA-protein crosslinks. Radiat. Res. 149, 543–549.

Damodar, D., D'Souza, U.J.A., Biswas, A., Bhat, S., 2012. Diazinon affects the cytoarchitecture of seminiferous epithelium in rat testis. Am. J. Biomed. Eng. 2, 13–16. https://doi.org/10.5923/j.ajbe.20120202.03.

Dasdag, S., Zulkuf Akdag, M., Aksen, F., Yılmaz, F., Bashan, M., Mutlu Dasdag, M., Salih Celik, M., 2003. Whole body exposure of rats to microwaves emitted from a cell phone does not affect the testes. Bioelectromagnetics 24, 182–188. https://doi.org/10.1002/bem.10083.

Ding, S.-S., Sun, P., Tian, H., Huo, Y.-W., Wang, L.-R., Han, Y., Zhang, Z., Liu, X., Xing, J.-P., 2018. Association between daily exposure to electromagnetic radiation from 4G smartphone and 2.45-GHz wi-fi and oxidative damage to semen of males attending a genetics clinic: a primary study. Int. J. Clin. Exp. Med. 11, 2821–2830. http://www.ijcem.com/files/ijcem0063001.pdf.

Douki, T., Bretonniere, Y., Cadet, J., 2000. Protection against radiation-induced degradation of DNA bases by polyamines. Radiat. Res. 153, 29–35.

Eghlidospour, M., Ghanbari, A., Mortazavi, S.M.J., Azari, H., 2017. Effects of radio-frequency exposure emitted from a GSM mobile phone on proliferation, differentiation, and apoptosis of neural stem cells. Anat. Cell Biol. https://doi.org/10.5115/acb.2017.50.2.115.

El-Kashlan, A.M., Nooh, M.M., Hassan, W.A., Rizk, S.M., 2015. Therapeutic potential of date palm pollen for testicular dysfunction induced by thyroid disorders in male rats. PLoS One 10, e0139493. https://doi.org/10.1371/journal.pone.0139493.

Ernst, E., 1989. A method for evaluation of epididymal sperm count and motility in the rat. Scand. J. Lab. Anim. Sci. 16, 67–71.

Foppiani, L., Schlatt, S., Simoni, M., Weinbauer, G.F., Hacker-Klom, U., Nieschlag, E.,

1999. Inhibin B is a more sensitive marker of spermatogenetic damage than FSH in the irradiated non-human primate model. J. Endocrinol. 162, 393–400.
Fragopoulou, A.F., Koussoulakos, S.L., Margaritis, L.H., 2010. Cranial and postcranial skeletal variations induced in mouse embryos by mobile phone radiation. Pathophysiol. Off. J. Int. Soc. Pathophysiol. 17, 169–177. https://doi.org/10.1016/j.pathophys.2009.10.002.
Ha, H.C., Sirisoma, N.S., Kuppusamy, P., Zweier, J.L., Woster, P.M., Casero, R.A., 1998. The natural polyamine spermine functions directly as a free radical scavenger. Proc. Natl. Acad. Sci. U. S. A. 95, 11140–11145.
Hancı, H., Kerimoğlu, G., Mercantepe, T., Odacı, E., 2018. Changes in testicular morphology and oxidative stress biomarkers in 60-day-old Sprague Dawley rats following exposure to continuous 900-MHz electromagnetic field for 1 h a day throughout adolescence. Reprod. Toxicol. 81, 71–78. https://doi.org/10.1016/j.reprotox.2018.07.002.
Holdcraft, R.W., Braun, R.E., 2004. Hormonal regulation of spermatogenesis. Int. J. Androl. 27, 335–342. https://doi.org/10.1111/j.1365-2605.2004.00502.x.
Holian, O., Astumian, R.D., Lee, R.C., Reyes, H.M., Attar, B.M., Walter, R.J., 1996. Protein kinase C activity is altered in HL60 cells exposed to 60 Hz AC electric fields. Bioelectromagnetics 17, 504–509. https://doi.org/10.1002/(SICI)1521-186X(1996)17:6<504::AID-BEM11>3.0.CO;2-K.
Hong, C.Y., Park, J.H., Ahn, R.S., Im, S.Y., Choi, H.-S., Soh, J., Mellon, S.H., Lee, K., 2004. Molecular mechanism of suppression of testicular steroidogenesis by proinflammatory cytokine tumor necrosis factor alpha. Mol. Cell. Biol. 24, 2593–2604. https://doi.org/10.1128/MCB.24.7.2593-2604.2004.
Imbert, V., Rupec, R.A., Livolsi, A., Pahl, H.L., Traenckner, E.B., Mueller-Dieckmann, C., Farahifar, D., Rossi, B., Auberger, P., Baeuerle, P.A., Peyron, J.F., 1996. Tyrosine phosphorylation of I kappa B-alpha activates NF-kappa B without proteolytic degradation of I kappa B-alpha. Cell 86, 787–798.
Jarabak, J., Adams, J.A., Williams-Ashman-Ashman, H.G., Talalay, P., 1962. Purification of a 17beta-hydroxysteroid dehydrogenase of human placenta and studies on its transhydrogenase function. J. Biol. Chem. 237, 345–357.
Kahsai, T.Z., Enders, G.C., Gunwar, S., Brunmark, C., Wieslander, J., Kalluri, R., Zhou, J., Noelken, M.E., Hudson, B.G., 1997. Seminiferous tubule basement membrane. Composition and organization of type IV collagen chains, and the linkage of alpha3(IV) and alpha5(IV) chains. J. Biol. Chem. 272, 17023–17032. https://doi.org/10.1074/JBC.272.27.17023.
Kaipia, A., Toppari, J., Mali, P., Kangasniemi, M., Alcivar, A.A., Hecht, N.B., Parvinen, M., 1990. Stage- and cell-specific expression of the ornithine decarboxylase gene during rat and mouse spermatogenesis. Mol. Cell. Endocrinol. 73, 45–52.
Kesari, K.K., Behari, J., 2012. Evidence for mobile phone radiation exposure effects on reproductive pattern of male rats: role of ROS. Electromagn. Biol. Med. 31, 213–222. https://doi.org/10.3109/15368378.2012.700292.
Kesari, K.K., Kumar, S., Behari, J., 2011. Effects of radiofrequency electromagnetic wave exposure from cellular phones on the reproductive pattern in male Wistar rats. Appl. Biochem. Biotechnol. 164, 546–559. https://doi.org/10.1007/s12010-010-9156-0.
Khan, A.U., Mei, Y.H., Wilson, T., 1992. A proposed function for spermine and spermidine: protection of replicating DNA against damage by singlet oxygen. Proc. Natl. Acad. Sci. U. S. A. 89, 11426–11427.
Krüger, A., Vowinckel, J., Mülleder, M., Grote, P., Capuano, F., Bluemlein, K., Ralser, M., 2013. Tpo1-mediated spermine and spermidine export controls cell cycle delay and times antioxidant protein expression during the oxidative stress response. EMBO Rep. 14, 1113–1119. https://doi.org/10.1038/embor.2013.165.
La Vignera, S., Condorelli, R.A., Vicari, E., Tumino, D., Morgia, G., Favilla, V., Cimino, S., Calogero, A.E., 2013. Markers of semen inflammation: supplementary semen analysis? J. Reprod. Immunol. 100, 2–10. https://doi.org/10.1016/j.jri.2013.05.001.
Lefèvre, P.L.C., Palin, M.F., Murphy, B.D., 2011. Polyamines on the reproductive landscape. Endocr. Rev. 32, 694–712. https://doi.org/10.1210/er.2011-0012.
Li, L., Rao, J.N., Bass, B.L., Wang, J.-Y., 2001. NF-κB activation and susceptibility to apoptosis after polyamine depletion in intestinal epithelial cells. Am. J. Physiol. Liver Physiol. 280, G992–G1004. https://doi.org/10.1152/ajpgi.2001.280.5.G992.
Livak, K.J., Schmittgen, T.D., 2001. Analysis of relative gene expression data using real-time quantitative PCR and the $2-\Delta\Delta CT$ method. Methods 25, 402–408. https://doi.org/10.1006/meth.2001.1262.
Lowry, O.H., Rosebrough, N.J., Farr, A.L., Randall, R.J., 1951. Protein measurement with the Folin phenol reagent. J. Biol. Chem. 193, 265–275.
Maheshwari, A., Misro, M.M., Aggarwal, A., Sharma, R.K., Nandan, D., 2009. Pathways involved in testicular germ cell apoptosis induced by H_2O_2 in vitro. FEBS J. 276, 870–881. https://doi.org/10.1111/j.1742-4658.2008.06831.x.
Mäkitie, L.T., Kanerva, K., Sankila, A., Andersson, L.C., 2009. High expression of antizyme inhibitor 2, an activator of ornithine decarboxylase in steroidogenic cells of human gonads. Histochem. Cell Biol. 132, 633–638. https://doi.org/10.1007/s00418-009-0636-7.
Manikonda, P.K., Rajendra, P., Devendranath, D., Gunasekaran, B., Channakeshava, Aradhya, R.S.S., Sashidhar, R.B., Subramanyam, C., 2007. Influence of extremely low frequency magnetic fields on Ca2+ signaling and NMDA receptor functions in rat hippocampus. Neurosci. Lett. 413, 145–149. https://doi.org/10.1016/j.neulet.2006.11.048.
Mohammed, H.S., Fahmy, H.M., Radwan, N.M., Elsayed, A.A., 2013. Non-thermal continuous and modulated electromagnetic radiation fields effects on sleep EEG of rats. J. Adv. Res. 4, 181–187. https://doi.org/10.1016/j.jare.2012.05.005.
Motawi, T.K., Abd Elgawad, H.M., Shahin, N.N., 2007. Modulation of indomethacin-induced gastric injury by spermine and taurine in rats. J. Biochem. Mol. Toxicol. 21, 280–288. https://doi.org/10.1002/jbt.20194.
Odacı, E., Özyılmaz, C., 2015. Exposure to a 900 MHz electromagnetic field for 1 hour a day over 30 days does change the histopathology and biochemistry of the rat testis. Int. J. Radiat. Biol. 91, 547–554. https://doi.org/10.3109/09553002.2015.1031850.
Okuma, Y., O'Connor, A.E., Muir, J.A., Stanton, P.G., de Kretser, D.M., Hedger, M.P., 2005. Regulation of activin A and inhibin B secretion by inflammatory mediators in adult rat Sertoli cell cultures. J. Endocrinol. 187, 125–134. https://doi.org/10.1677/joe.1.06266.
Opuwari, C.S., Henkel, R.R., 2016. An update on oxidative damage to spermatozoa and oocytes. Biomed. Res. Int. 2016, 9540142. https://doi.org/10.1155/2016/9540142.
Paffi, A., Merla, C., Pinto, R., Lovisolo, G.A., Liberti, M., Marino, C., Repacholi, M., Apollonio, F., 2013. Microwave exposure systems for in vivo biological experiments: a systematic review. IEEE Trans. Microw. Theory Tech. 61, 1980–1993. https://doi.org/10.1109/TMTT.2013.2246183.
Paglia, D.E., Valentine, W.N., 1967. Studies on the quantitative and qualitative characterization of erythrocyte glutathione peroxidase. J. Lab. Clin. Med. 70, 158–169.
Pall, M.L., 2018. Wi-Fi is an important threat to human health. Environ. Res. 164, 405–416. https://doi.org/10.1016/j.envres.2018.01.035.
Parker, M.T., Gerner, E.W., 2002. Polyamine-mediated post-transcriptional regulation of COX-2. Biochimie 84, 815–819.
Paul, S., Kang, S.C., 2013. Natural polyamine inhibits mouse skin inflammation and macrophage activation. Inflamm. Res. 62, 681–688. https://doi.org/10.1007/s00011-013-0620-5.
Pegg, A.E., 2014. The function of spermine. IUBMB Life 66, 8–18. https://doi.org/10.1002/iub.1237.
Peltola, V., Huhtaniemi, I., Ahotupa, M., 1992. Antioxidant enzyme activity in the maturing rat testis. J. Androl. 13, 450–455.
Pulkkinen, P., Sinervirta, R., Jänne, J., 1975. Modification of the metabolism of rat epididymal spermatozoa by spermine. Biochem. Biophys. Res. Commun. 67, 714–722.
Rao, B., Soufir, J.C., Martin, M., David, G., 1989. Lipid peroxidation in human spermatozoa as related to midpiece abnormalities and motility. Gamete Res. 24, 127–134. https://doi.org/10.1002/mrd.1120240202.
Rato, L., Alves, M.G., Dias, T.R., Lopes, G., Cavaco, J.E., Socorro, S., Oliveira, P.F., 2013. High-energy diets may induce a pre-diabetic state altering testicular glycolytic metabolic profile and male reproductive parameters. Andrology 1, 495–504. https://doi.org/10.1111/j.2047-2927.2013.00071.x.
Santini, S.J., Cordone, V., Falone, S., Mijit, M., Tatone, C., Amicarelli, F., Di Emidio, G., 2018. Role of Mitochondria in the Oxidative Stress Induced by Electromagnetic Fields: Focus on Reproductive Systems 2018. https://doi.org/10.1155/2018/5076271.
Schrans-Stassen, B.H.G.J., van de Kant, H.J.G., de Rooij, D.G., van Pelt, A.M.M., 1999. Differential expression of c- kit in mouse undifferentiated and differentiating type A spermatogonia. Endocrinology 140, 5894–5900. https://doi.org/10.1210/endo.140.12.7172.
Sepehrimanesh, M., Kazemipour, N., Saeb, M., Nazifi, S., 2014a. Analysis of rat testicular proteome following 30-day exposure to 900 MHz electromagnetic field radiation. Electrophoresis 35, 3331–3338. https://doi.org/10.1002/elps.201400273.
Sepehrimanesh, M., Saeb, M., Nazifi, S., Kazemipour, N., Jelodar, G., Saeb, S., 2014b. Impact of 900 MHz electromagnetic field exposure on main male reproductive hormone levels: a Rattus norvegicus model. Int. J. Biometeorol. 58, 1657–1663. https://doi.org/10.1007/s00484-013-0771-7.
Sepehrimanesh, M., Kazemipour, N., Saeb, M., Nazifi, S., Davis, D.L., 2017. Proteomic analysis of continuous 900-MHz radiofrequency electromagnetic field exposure in testicular tissue: a rat model of human cell phone exposure. Environ. Sci. Pollut. Res. Int. 24, 13666–13673. https://doi.org/10.1007/s11356-017-8882-z.
Setyawan, E.M.N., Kim, M.J., Oh, H.J., Kim, G.A., Jo, Y.K., Lee, S.H., Choi, Y. Bin, Lee, B.C., 2016. Spermine reduces reactive oxygen species levels and decreases cryocapacitation in canine sperm cryopreservation. Biochem. Biophys. Res. Commun. 479, 927–932. https://doi.org/10.1016/j.bbrc.2016.08.091.
Shah, G.V., Sheth, A.R., Mugatwala, P.P., Rao, S.S., 1975. Effect of spermine on adenyl cyclase activity of spermatozoa. Experientia 31, 631–632.
Shahin, N.N., Mohamed, M.M., 2017. Nano-sized titanium dioxide toxicity in rat prostate and testis: possible ameliorative effect of Morin. Toxicol. Appl. Pharmacol. 334, 129–141. https://doi.org/10.1016/j.taap.2017.08.014.
Singh, N.P., McCoy, M.T., Tice, R.R., Schneider, E.L., 1988. A simple technique for quantitation of low levels of DNA damage in individual cells. Exp. Cell Res. 175, 184–191.
Solek, P., Majchrowicz, L., Bloniarz, D., Krotoszynska, E., Koziorowski, M., 2017. Pulsed or continuous electromagnetic field induce p53/p21-mediated apoptotic signaling pathway in mouse spermatogenic cells in vitro and thus may affect male fertility. Toxicology 382, 84–92. https://doi.org/10.1016/j.tox.2017.03.015.
Spotheim-Maurizot, M., Ruiz, S., Sabattier, R., Charlier, M., 1995. Radioprotection of DNA by polyamines. Int. J. Radiat. Biol. 68, 571–577.
Talalay, P., 1962. Hydroxysteroid dehydrogenase. In: Colowick, S., Kaplan, N. (Eds.), Methods in Enzymology. Academic Press, New York, pp. 512–516.
Tanimoto, K., Yoshida, E., Mita, S., Nibu, Y., Murakami, K., Fukamizu, A., 1996. Human activin betaA gene. Identification of novel 5′ exon, functional promoter, and enhancers. J. Biol. Chem. 271, 32760–32769.
Uchiyama, M., Mihara, M., 1978. Determination of malonaldehyde precursor in tissues by thiobarbituric acid test. Anal. Biochem. 86, 271–278. https://doi.org/10.1016/0003-2697(78)90342-1.
Uckun, F.M., Kurosaki, T., Jin, J., Jun, X., Morgan, A., Takata, M., Bolen, J., Luben, R., 1995. Exposure of B-lineage lymphoid cells to low energy electromagnetic fields stimulates Lyn kinase. J. Biol. Chem. 270, 27666–27670.
Valberg, P.A., van Deventer, T.E., Repacholi, M.H., 2007. Workgroup report: base stations and wireless networks-radiofrequency (RF) exposures and health consequences. Environ. Health Perspect. 115, 416–424. https://doi.org/10.1289/ehp.9633.
Wang, X., Ikeguchi, Y., McCloskey, D.E., Nelson, P., Pegg, A.E., 2004. Spermine synthesis is required for normal viability, growth, and fertility in the mouse. J. Biol. Chem. 279, 51370–51375. https://doi.org/10.1074/jbc.M410471200.
Wei, C., Wang, Y., Li, M., Li, H., Lu, X., Shao, H., Xu, C., 2016. Spermine inhibits endoplasmic reticulum stress - induced apoptosis: a new strategy to prevent cardiomyocyte apoptosis. Cell. Physiol. Biochem. 38, 531–544. https://doi.org/10.1159/000438648.
Wu, S., Razavi, B., 1998. A 900-MHz/1.8-GHz CMOS receiver for dual-band applications. IEEE J. Solid-State Circuits 33, 2178–2185. https://doi.org/10.1109/4.735702.